



AME0016

Investigation of horizontal-axis wind turbine wake phenomena

Ryo Amano*, R.S. Jackson

University of Wisconsin-Milwaukee, 115 E. Reindl Way, Glendale, WI 53212, U.S.A.

*Corresponding Author: amano@uwm.edu

Abstract. The advancement of wind energy as an alternative source of hydrocarbons depends heavily on research activities in simulation technique and experimentation. The wake behind wind turbines affects the power output and efficiency of a wind farm. Being able to simulate the wake dynamics of a wind turbine efficiently may result in optimum spacing, longer wind turbine life, and quicker payback on the wind farm investment.

1. Introduction

Wind power has been shown to be one of the most viable sources of renewable energy. The technology is mainly due to recent technological advances that have lowered the price of wind energy to a level that is competitive with more conventional means of producing energy. The blades of a wind turbine are an important component of the machine and thus have been the subject of much research. Most commercial blade designs incorporate a straight edge span-wise profile with airfoil cross-sections of various sizes and orientations. The configuration of these parameters usually follows guild lines resulting from well-established theory. If these blades are designed correctly, they can be very efficient. To increase this efficiency, some manufacturers have experimented with different profile geometries. One common alteration that has been seen is a swept edge profile, such as that found in the Skystream 3.7 turbine[1]. The advantages and disadvantages associated with this shape are not well documented due to the complex nature of airflow around a rotating blade and the numerical investigation that is required.

Traditionally, analytical methods employing the blade element momentum (BEM) theory have been used to analyze wind turbine blade performance [2]. The BEM method treats a given cross-section of a turbine blade as an independent airfoil. Based on the rotation rate, oncoming wind speed and spanwise position of the cross-section, an appropriate chord length and angle of twist can be specified. Once several cross-section configurations are defined, the overall performance of the blade can be estimated by indexing previously determined 2D lift, drag, and moment data. These methods are efficient and reasonably accurate for an initial design, but since each cross-section is considered independent and the data used to determine its performance in 2D, involved 3D flow effects are not directly taken into account [3]. For this reason, many researchers have to look to computational fluid dynamics to supplement their design process.

Bak et al. [4] explored the possibility of extracting force data from CFD simulations to enhance existing 2-D airfoil data. This data could then be used with the blade element momentum theory or actuator blade approach to determine wind turbine performance analytically. The turbine used in the simulations of this study is the NTK500/41 with LM19.1 blades [5]. The computational domain consisted of a third of the flow volume of the entire rotor taking advantage of the symmetry at every 120° intervals. With this approach, only a single blade needs to be simulated.

2. Experimental Setup

The wind tunnel in the Wind Energy Laboratory at the University of Wisconsin-Milwaukee (UWM) was used for the experimental study. A photograph of the wind tunnel is shown in Figure 1. Welsh [6] provides a detailed description of the wind tunnel facility and the design considerations, but a general synopsis is provided here. The wind tunnel at UWM is an open-circuit, suction type tunnel that uses an axial fan to draw air through the test section. The inlet settling chamber section was designed with a 7.62 cm long honeycomb and 1 cm hexagonal shaped cells to reduce the large-scale turbulence and to eliminate mean lateral and vertical velocity components. A series of screens with reduced mesh sizes was incorporated to reduce further the turbulence and lessen the variation in the average longitudinal velocity.

The room is temperature controlled which reduces the change in temperature during testing. Temperature changes with the wind turbine operating continuously for up to 10 hours were less than 0.5 C. The inlet to the contraction section is a bit over 9.3 square meters and transitions to the 1.4 rectangular meter tests section in ~4 m distance. The 6.2 contraction ratio is on the low-end of the recommended range, but given the low wind tunnel speed, it was deemed acceptable. The test section is ~120 cm × 120 cm × 243 cm long and has clear polycarbonate walls to provide a smooth surface. The wind tunnel boundary layer was not measured for this experimentation, but it was estimated to be less than 15 cm in 2.4 m so that the boundary layer does not extend into the turbine wake. The diffuser section was designed with a 2.25 expansion ratio and a 2.5° expansion angle. The diffuser section transitions from a square cross-section at the exit of the test section to an octagonal shape at the entrance to the 1.83 m fan diameter. A rubber coupling was installed between the diffuser and the fan to reduce vibration and prevent measurement errors. The six-bladed fan is attached to a 34 hp motor which is controlled by a variable frequency motor speed drive mounted to the side of the fan enclosure. The motor frequency and resulting wind speed were established during this experimentation.

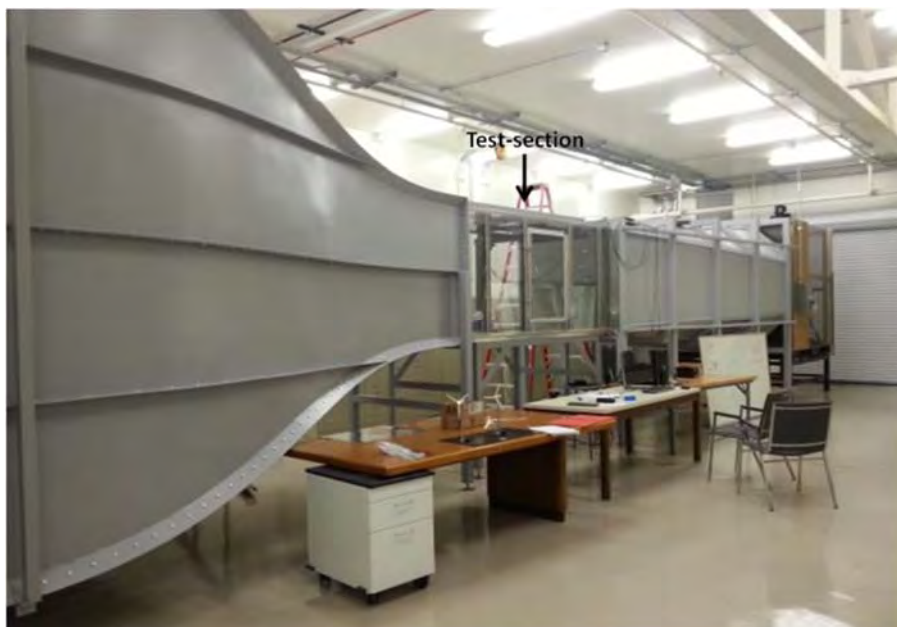


Figure 1. Wind Tunnel Test Facility.

3. Results

The calibration procedure for the surface interpolation technique was identical to the polynomial surface fit method, and the same datasets were used for all comparisons. Since the griddata.m function uses the exact calibration points in the interpolation, an error analysis at those points resulted in zero error. To evaluate and compare methods, 15 of the 45 velocity values were selected overall yaw angles to establish the calibration surfaces, and 15 intermediate velocity values were used to compute the normalized standard deviation, ε_N . Figure 2 shows the points used for building the calibration grid, and also the points (different velocity settings) used to evaluate ε_N .

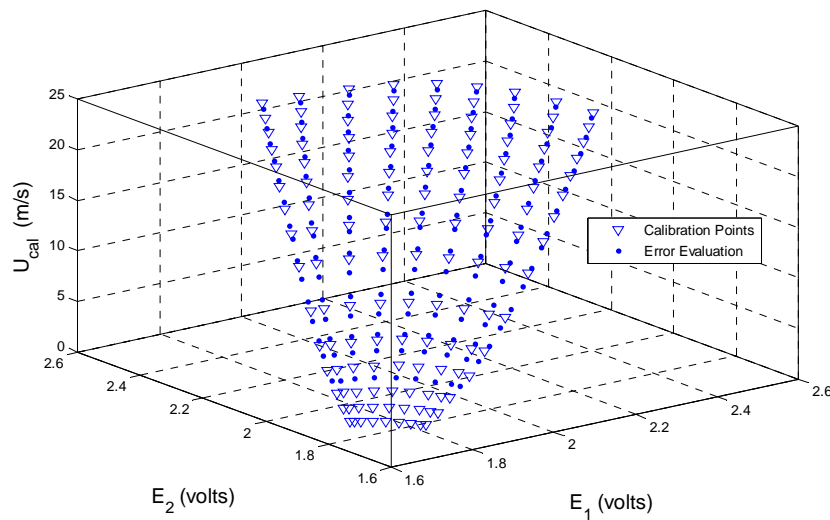


Figure 2. Points used to develop calibration surfaces and locations used for error evaluation.

Table 1 shows the computed normalized standard deviation, ε_N , for the different calibration methods at all yaw angles along with the computation time for converting the voltages to velocities. The values of ε_N are plotted for each procedure in Figure 3 to provide a visual comparison.

Table 1. Comparison of normalized standard deviation, yaw angle error, and computation time for different calibration methods.

Yaw Angle [deg]	Effective Angle		Polynomial Surface Fit		Surface Interpolation	
	ε_N	t_{comp} [msec]	ε_N	t_{comp} [msec]	ε_N	t_{comp} [msec]
-40	0.169	5.05	0.243	0.75	0.234	51.1
-30	0.105	5.11	0.125	0.73	0.134	49.9
-20	0.048	4.84	0.044	0.93	0.060	52.4
-10	0.010	4.93	0.004	0.91	0.016	54.4
0	0.006	4.99	0.009	0.91	0.008	49.8
10	0.010	5.22	0.004	0.87	0.015	48.0
20	0.089	4.95	0.076	0.90	0.060	51.2
30	0.156	4.98	0.149	0.87	0.114	51.6
40	0.210	5.00	0.213	0.91	0.234	55.3
Average	0.089	5.01	0.096	0.86	0.097	51.52

From Figure 3, it is clear that the accuracy of the velocity measurement is dependent on the yaw angle regardless of which method is used. More importantly, the biharmonic interpolation method is shown to be as accurate as either of the more traditional effective angle or polynomial surface fit methods.

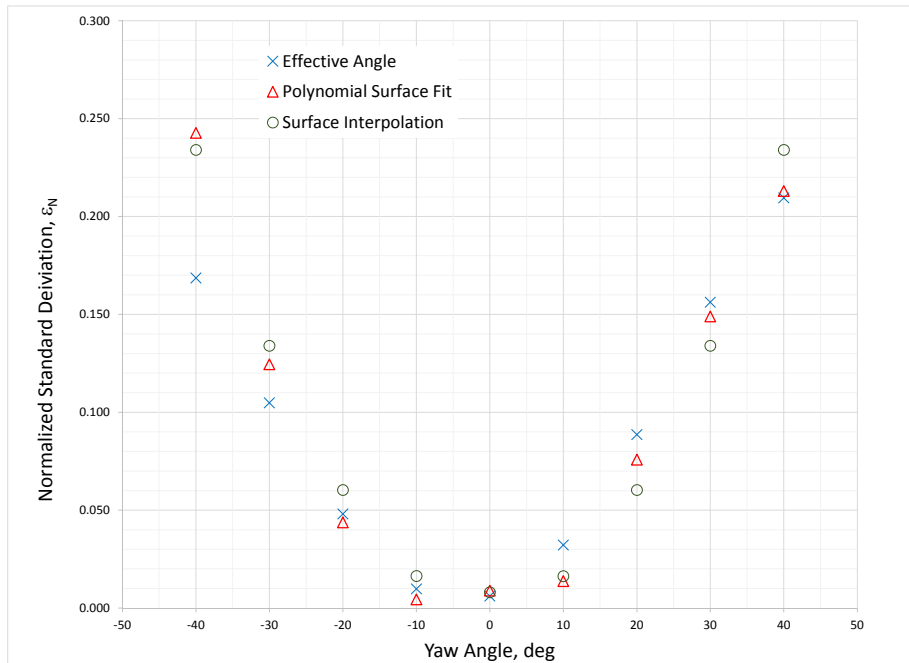


Figure 3. Comparison of normalized standard deviation for different hotwire calibration methods.

Converting voltages to velocity can be time-consuming, especially for large file sizes and copious data files. The Matlab tic and toc commands were used to estimate the time for converting the voltages to velocity and computing ϵ_N . The computation was performed on a 64-bit Windows Operating System with an Intel i7-3635QM processor and 16 GB of RAM. All coefficients determined the computation time and grid calibration values were loaded. The results show that the computation time using the griddata.m function was substantially longer than either the polynomial surface fit or capable angle method while the polynomial surface fit method is an order of magnitude faster than the effective angle method. The main advantage of using the surface interpolation technique was its simplicity to implement; it was one command line of programming. The polynomial surface fit technology was mathematically rigorous and required a bit more programming ingenuity; however, the efficiency of the script made it computationally faster.

Another advantage of using the polynomial surface fit or surface interpolation method comes in reducing the uncertainty due to the hot wire probe angle when taking measurements in the wind tunnel. Before wind tunnel measurements, the 54H10 calibrator was placed in the wind tunnel with the axis of the nozzle aligned with the axis of the wind tunnel and the nozzle perpendicular to the probe support as shown in Figure 4.

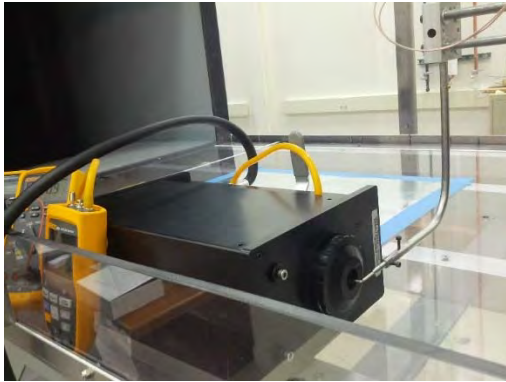


Figure 4. In-situ calibration of hot wire anemometer.

In almost every instance before starting wind tunnel experiments, plotting the in-situ calibration with the full calibration data indicated a slight misalignment of the probe, as shown in . The probe angle was then adjusted such that the in-situ calibration matched the full calibration.

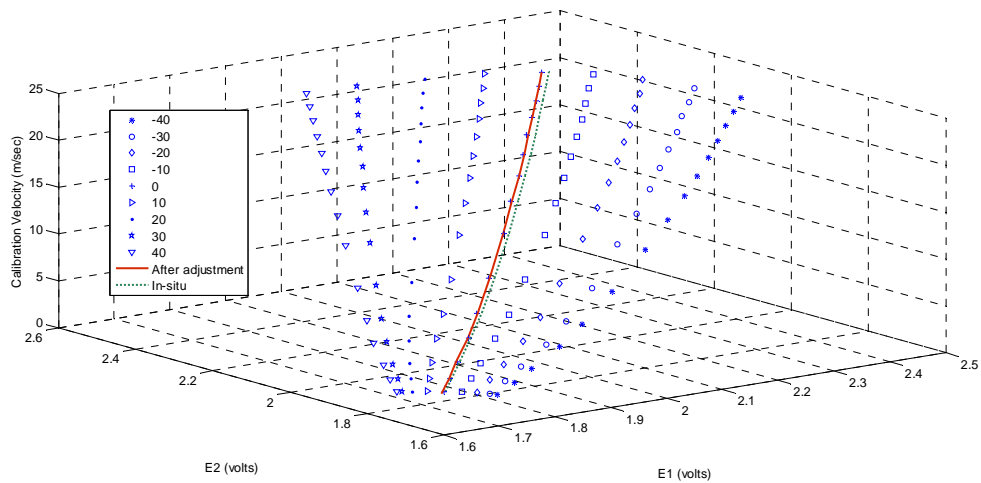


Figure 5. In-situ calibration correction for probe angle

Moving downstream and further and into the far-wake region ($x/D_b > 1$), the experimental data shows a trend toward an axisymmetric Gaussian profile.

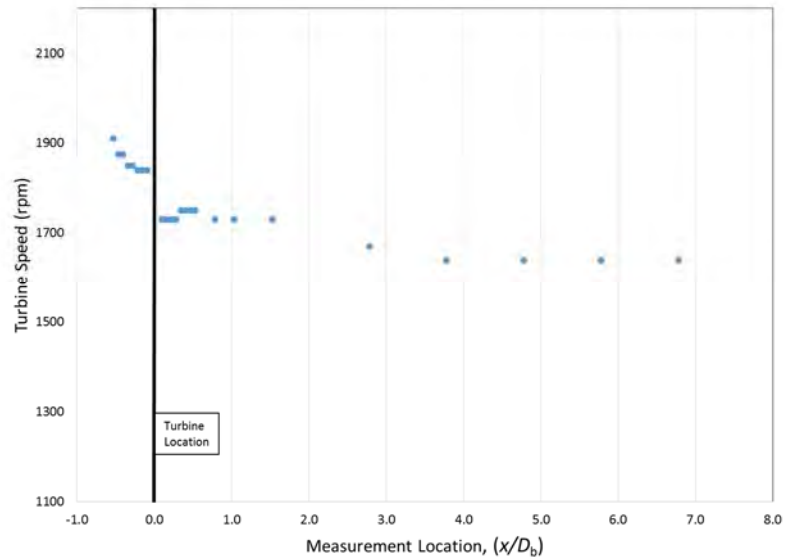


Figure 6. Measured blade speed with hot-wire probes positioned at the hub height.

Figure 6 shows the closer the traverse arm is to the turbine, the higher the rotational speed. The highest rotational speeds occurred when the traverse arm was even or ahead of the turbine. The position of the traverse arm in the lateral direction also affected the blade speed, but the effect was not documented. The rotational speed increase is caused by more airflow to the turbine as it is re-directed around the traverse arm and the area between the turbine and the traverse is reduced; this effect was also seen in measurements with multiple turbines.

Figure 7 shows the profile at locations up to the end of the near-wake region ($x/D_b < 1$). The RSM turbulence model appears to overpredict the deficit from the rotor and the tower for all methods in this region; however, the shape of the RBM profile is a better match to the experimental measurements.

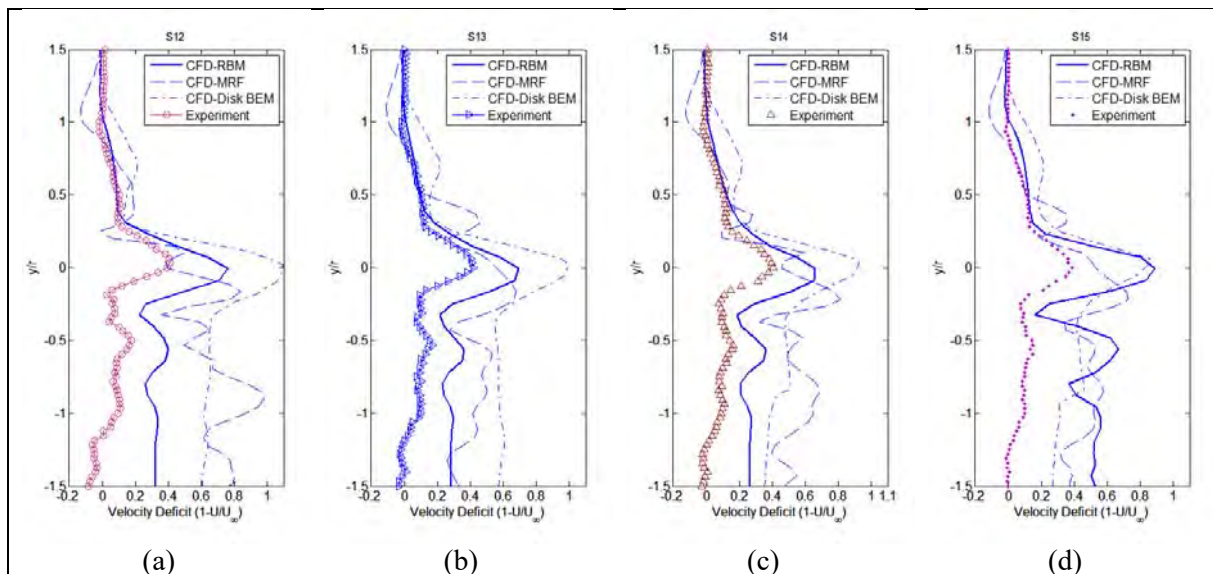


Figure 7. Comparison of velocity deficit to experimental data at several vertical measurement planes using different CFD modeling methods: (a) S12 (b) S13 (c) S14 (d) S15, $U_\infty=6.60$ m/s, traverse arm positioned at $x/D_b \sim 8$.

4. Conclusions

A hot-wire calibration comparison showed that using a surface interpolation technique to linearize the hot-wire voltage to velocity may be more accurate than sufficient angle or polynomial surface fit methods. The method was computationally more expensive when considering large files are a large number of records. The velocity deficit measurements showed excellent repeatability considering size planes upstream of the first turbine and between the first and second turbine. The hot-wire measurements showed the dissipation of turbulence intensity and erosion of the velocity deficit were consistent with theory and prior research. The experimental results highlighted the influence of traverse and future experiments in the wind tunnel will need to consider how the hot-wire probe is supported and crossed during measurements. Factors that may have influenced the experimental results include the position and orientation of the turbine blades and the surface quality of the wind turbine blades.

Reference

- [1] Southwest Windpower., www.windenergy.com
- [2] Vermeer, L., Sørensen, J., Crespo, A., 2003 "Wind Turbine Wake Aerodynamics" Progress in Aerospace Science; Vol. 39; 467-510.
- [3] Hansen, MOL., 2000 "Aerodynamics of Wind Turbines. Rotors, Load and Structures"; James&James, London
- [4] Bak, C., Fuglsang, P., Sorensen, N., Madsen, H., Shen, W., Sorensen, J., 1999 "Airfoil Characteristics for Wind Turbines" Riso-R-1065(EN)
- [5] Sørensen, N.N., 2002, "Transition Prediction on the NORDTANK 500/41 Turbine Rotor," Risø-R-1365, Risø National Laboratory, Roskilde.
- [6] A. Welsh, "Low turbulence wind tunnel design and wake characterization," University of Wisconsin Milwaukee Digital Commons-Theses and Dissertations, Milwaukee, WI, 2013.